SPE 59372

Support-Operators Method in the Identification of Permeability Tensor Orientation

Dmitriy B. Silin[1], and Tad W. Patzek[1,2,3]

[1]Lawrence Berkeley National Laboratory; [2]University of California at Berkeley; [3]SPE Member, patzek@patzek.berkeley.edu

This paper was prepared for presentation at the 2000 SPE/DOE Improved Oil Recovery Symposium held in Tulsa, Oklahoma, 3–5 April 2000.

Abstract

The dependence of rock permeability on direction, or permeability anisotropy, is confirmed by numerous field examples. Ability to measure permeability anisotropy is very important for correct placement of wells. There exist several methods of identifying the maximum and minimum permeability coefficients by interpreting specially designed well tests. Here we develop a new method of estimating the angle of orientation of permeability tensor. We assume that the principal permeabilities near a cored or otherwise logged well are already known. Based on this information we develop a method of estimating the angle of permeability tensor orientation away from the well. To accomplish this task we need pressure measurements in monitoring wells.

The orientation of permeability tensor is identified by minimizing the square of the differences between measured and computed data. The underlying boundary-value problem is discretized by the support-operators method, which imposes few restrictions on the grid structure; produces a conservative finite-difference scheme; and can be applied to very heterogeneous systems. The gradient and second differential of the minimization criterion are obtained through two systems of adjoint equations, called the first and second adjoint systems. The gradient of the criterion is obtained both in continuous and discrete versions. As an illustration, we analyze a steady state isothermal, single-phase pressure equation in a heterogeneous porous medium. A few applications of the technique developed in this paper for rectangular and curvilinear grids confirm good performance of the algorithm.

Introduction

Often, when modeling fluid flow in a porous rock, it is assumed that permeability of the rock is isotropic, i.e. the permeability coefficient is the same regardless of the direction of pressure gradient. In other words, the direction of flow is aligned with the pressure gradient. This simplifying assumption cannot be accepted in every case. For example, the permeability of fissured rock is substantially dependent on micro-fractures; hence, the dominating orientation of the fractures can make the direction of flow different from that of the pressure gradient. Non-isotropic properties of a sedimentary formation can result from history of sedimentation. For example, the formation may dip or it may contain a buried riverbed.

Occurrences of anisotropy in oil reservoirs have been well documented, e.g.[1, 2]. Romm[3] provides several field examples where measurements indicate the dependence of permeability on direction. Another field example with comprehensive well test data analysis is given in Ref.[4]. The ratio of the maximum to the minimum permeability can be as large as 10^3. More references related to the studies of anisotropy of permeability in fractured reservoirs can be found in Ref.[5].

Clearly, an understanding of permeability anisotropy is very important, for instance, in drilling new wells in correct locations. There exist several techniques for analyzing permeability anisotropy. Some techniques rely on modifications of injection-production models and respective well-test procedures and estimate permeability by matching well-test data. Although there is no consensus on which model is better[6], the common idea is to match the data by an appropriate choice of the maximum and minimum permeability coefficient and appropriate orientation of the permeability tensor. In Ref.[5], the authors develop techniques to estimate the principal values of non-isotropic permeability tensor using single well-test data.

In the present paper, we assume that the principal permeabilities near a well are already known. Based on this

information we develop a method of estimating the angle of permeability tensor orientation away from the well. To accomplish this task we need pressure measurements monitoring wells. Although the illustrative examples below are simplistic, the method we develop here can be applied in a much more general situation. The main components of the algorithm are the computation of the gradient of the minimized functional through the adjoint system of equations and solution of the respective boundary-value problems using the method of support operators. The latter is a powerful finite-difference method producing conservative discretization of differential equations with full permeability tensor on a practically arbitrary grid. Our choice of the support-operators method was also encouraged by the fact that the resulting discrete equations have a form that is very convenient for deriving the discrete version of the adjoint system, see Appendix D below. Other methods of discretization often lead to cumbersome calculations of unobservable parameters.

The paper is organized as follows. After formulating the underlying boundary-value problem, we construct its discretization via the method of support operators. Then we formulate an identification problem and obtain first and second differentials of the minimization criterion via first and second adjoint system. We develop an algorithm of minimization of the functional and apply this algorithm on rectangular and curvilinear meshes. Although we avoid going deeply into all the technical details of calculations, the principal derivations are outlined in four appendices.

Problem Statement

Our main objective is to demonstrate the method rather than to analyze specific data. Therefore, we formulate the problem in a simplified form. Namely, we consider a steady state pressure equation

$$\nabla \cdot (K\nabla p) = -f \ , \ldots\ldots\ldots\ldots (x, y) \in \Omega \ , \ldots\ldots\ldots\ldots (1)$$

subject to the Dirichlet boundary condition

$$p\big|_{\Gamma} = \phi \ . \ldots\ldots\ldots\ldots\ldots\ldots\ldots\ldots\ldots\ldots\ldots\ldots (2)$$

Here Ω is a two-dimensional domain and Γ is its boundary $\partial\Omega$, where the values of the pressure are characterized by a known function ϕ. Under these assumptions, Eq. (1) is a steady-state single-phase pressure equation[7]. The function f characterizes the rate of injection or production, depending on the type of well we are looking at. In order to simplify the calculations further, it is assumed that the right-hand side of Eq. (1) is multiplied by the constant viscosity of the fluid. Again, we are using this simple model just to demonstrate a technique of finding the orientation of permeability tensor, which can be applied in a more general case without major changes. We only require that the domain Ω is reasonably regular, and assume that K, the permeability tensor to be identified, is constant. We also suppose that tensor K is symmetric and positive definite and its principal values, k_1 and k_2, are already known. In that case, K equals a rotation of the diagonal tensor $\begin{matrix} k_1 & 0 \\ 0 & k_2 \end{matrix}$ and our goal is to estimate the rotation angle θ.

From the problem statement, the traditional finite-difference techniques will clearly not work equally well in our case. Indeed, we have to deal with a domain of general shape and take into account that the permeability tensor may have off-diagonal elements. Therefore, we first discretize the boundary-value problem (1)-(2) using the support-operators method on a grid of an arbitrary shape. Second, we formulate the optimization problem of identification of the rotation angle θ. As we demonstrate, the support-operators method is very natural for solving both the forward and the adjoint problems. Finally, we present a few computational examples.

Support-Operators Method

The support-operators method was introduced in the early 80's in the works by Shashkov, Samarski and others[8, 9]. The main idea is that discretization should reflect the principle properties of the original boundary-value problem. In particular, we recall that Eq. (1) combines two balance equations: the mass balance and the momentum balance, i.e., Darcy's law[7]. The mass balance equation can be expressed in terms of a divergence operator, whereas the momentum balance equation is formulated using a flux operator, which is $K\nabla p$ in Eq. (1). The divergence and the flux operators are related to each other through the Gauss-Ostrogradski divergence theorem[10, 11]. In fact, divergence and flux are differential operators adjoint to each other. This implies that the discretization of divergence and flux, in order to adequately reflect the properties of the boundary-value problem (1)-(2), should satisfy a discrete analog of the Gauss-Ostrogradski equality. The support-operators method appropriately takes into account all these considerations and the discrete approximation of the Laplace operator on the left-hand side of Eq. (1) is provided by a symmetric positive definite matrix. Moreover, the operator representations in the method are coordinate independent and can be applied practically on any domain and on any grid. Many discretization techniques not based on finite elements impose strict requirements on the orientation of grid blocks with respect to the flow direction[12-14]. It is very difficult to satisfy these grid orientation requirements unless the solution is approximately known beforehand. The support-operators method does not impose such requirements. This method is based on the Gauss-Ostrogradski divergence theorem, which establishes a duality between the divergence and flux operators. The resulting finite difference scheme preserves this duality.

Assume that domain Ω is discretized with grid Ω_h, made of convex quadrilateral cells. We assume quadrilateral cells for consistency with "regular" 5-point or 9-point stencils on a rectangular 2D grid. A more natural discretization in 2D would involve triangular or hexagonal cells. Denote by u a discrete array approximating the solution p of Eqs. (1)-(2). In each interior cell of grid Ω_h, u is equal to p evaluated at the centroid of the respective cell. At the boundaries of Ω_h, the function p is evaluated in the middle of the edge (edges, for the corner cells) lying on the boundary of Ω_h. We assume that the 2D grid Ω_h has $N_x \times N_y$ quadrilateral cells, enumerated by indices i, j, $1 \le i \le N_x$, $1 \le j \le N_y$. The same indexing is applied to the array u in the interior cells. At the boundary, we shift the respective index by one half. For example, the values of u related to the left boundary have indices $u_{1/2\,j}$, as shown in **Fig. 1**.

Following[8, 9], we characterize flux through each cell by four numbers f_{ij}^{ν}, $\nu = 1,2,3,4$, the normal components of the fluxes through the boundaries of the cell, see Fig. 2. The positive orientation of the flow is north and east, so that fluxes $f_{ij}^{1,4}$ are evaluated along the inward normals, whereas fluxes $f_{ij}^{2,3}$ are evaluated along the outer normals. Denote by w the array of vectors characterizing the flux at the corners of the cells. Since, in general, the flux may be discontinuous, the value of w at the same vertex may be different in different cells. In other words, w may take up to four different values at each vertex. The relation between the arrays f and w is established through matrix Φ, see Appendix A for details.

In Appendix A, we briefly outline discretizations of divergence and an integral equality asserted by the Gauss-Ostrogradski theorem. The formulae we obtain are Eqs. (A-6) and (A-17). In particular, Eq. (A-17) implies that for an arbitrary array of fluxes f the following equality holds true:

$$\Phi^* \mathcal{K}^{-1} B \Phi \mathcal{L} u \cdot f = -DIV^* \Lambda u \cdot f + \Lambda_b u_b \cdot f_b \quad \text{....(3)}$$

The matrices in Eq. (3) are defined in Appendix A. Here we remark that matrix $\mathcal{K}^{-1} B$ is symmetric positive definite and matrix Λ is diagonal with positive elements on the main diagonal. In addition, we put

$$\Lambda_b u_b \cdot f_b = \sum_{j=1}^{N_y} u_{1/2\,j} f_{1\,j}^1 l_{1\,j}^1 + u_{N_x+1/2\;\,j} f_{N_x j}^3 l_{N_x j}^3 + \sum_{j=1}^{N_y} u_{i1/2} f_{i1}^4 l_{i1}^4 + u_{i\,N_y+1/2} f_{iN_y}^2 l_{iN_y}^2 \quad \text{.....(4)}$$

Here l_{ij}^{ν}, $\nu = 1,2,3,4$, are the lengths of the edges of cell (i,j). Eq. (4) involves only the boundary values of u and f. Since we deal with a Dirichlet boundary-value problem, the boundary values of u are equal to the respective values of function ϕ, see Eq. (2). Due to the arbitrariness of f, Eq. (3) implies that

$$\mathcal{L} u = -\Phi^* \mathcal{K}^{-1} B \Phi^{-1} DIV^* \Lambda u + \Phi^* \mathcal{K}^{-1} B \Phi^{-1} \Lambda_b u_b \quad \text{.(5)}$$

Equation (5) provides the discretization of the flux operator $K\nabla p$ on grid Ω_h dual to the discretization of the divergence DIV in Eq. (A-6). In general, the product $\Phi^* \mathcal{K}^{-1} B \Phi$ is a five-diagonal positive definite sparse matrix. For the case of rectangular grid and diagonal permeability tensor, it can be shown that matrix $\Phi^* \mathcal{K}^{-1} B \Phi$ is diagonal and $\Phi^* \mathcal{K}^{-1} B \Phi^{-1} DIV^* \Lambda$ is a banded sparse matrix. Its structure is shown in **Fig. 3**.

In order to construct a discretization of the boundary-value problem (1)-(2), we take the superposition of the discretized divergence (A-6) and flux operator (3):

$$-DIV\ \Phi^* \mathcal{K}^{-1} B \Phi^{-1} DIV^* \Lambda u = -F + \Phi^* \mathcal{K}^{-1} B \Phi^{-1} \Lambda_b u_b \quad \text{.(6)}$$

Applying the diagonal matrix Λ to both sides of Eq. (6), we obtain the following system of linear equations

$$\mathcal{A} u = \mathbf{b} \quad \text{.....(7)}$$

where

$$\mathcal{A} = \Lambda DIV\ \Phi^* \mathcal{K}^{-1} B \Phi^{-1} DIV^* \Lambda \quad \text{.....(8)}$$

and

$$\mathbf{b} = F - \Phi^* \mathcal{K}^{-1} B \Phi^{-1} \Lambda_b u_b \quad \text{.....(9)}$$

Clearly, from Eq. (8) it follows that matrix $\mathcal{A}$ is symmetric and positive definite, regardless of whether the grid is rectangular or not. It is possible to prove that if the grid is rectangular and the permeability tensor K has zero off-diagonal elements, then matrix $\mathcal{A}$ has the same five-diagonal structure as the matrix produced by a standard finite difference scheme on a 5-point stencil[8, 9], see **Fig. 4**. At the same time, if the grid is either irregular or the off-diagonal elements of the permeability tensor are nonzero, both matrices $\mathcal{L}$ and $\mathcal{A}$ are full.

Identification problem

Assume that the solution to the boundary-value problem (1)-(2) is known at a point or points. In other words, pressure measurements are available at certain points of domain Ω. Then our goal is to find a permeability tensor such that the numerical solution to (1)-(2) matches the measurements. Mathematically the problem can be formulated in the following way: find the permeability tensor K minimizing the performance criterion

$$J[K] = \frac{1}{2}\int_{\Omega} w(x,y)\ \left(p(x,y) - p_*(x,y)\right)^2 d\Omega \quad \text{.....(10)}$$

subject to constraints (1)-(2). Here $w(x,y)$ is a nonnegative weight function, $p_*(x,y)$ is the target function characterizing the results of measurements. If measurements are available only at one or several isolated points with coordinates (x_i, y_i), i=1,2,...,N, then we put

$$w(x,y) = \sum_{i=1}^{N} \delta\ (x - x_i,\ y - y_i) \quad \text{,.....(11)}$$

where δ is Dirac's delta-function, and the values of the target function outside points x_i, y_i do not matter. More generally, the values of $p_*(x,y)$ do not matter wherever $w(x,y) = 0$.

For numerical minimization of functional (10), we have to calculate its gradient, i.e., the linear part of its variation under a perturbation of the permeability tensor $K \to K + \delta K$. In Appendix B, we obtain that the gradient of functional (10) is equal to

$$\delta J = \int_{\Omega} -\nabla\psi \cdot (\delta K \nabla p)\, d\Omega \quad \text{.....(12)}$$

where $\psi(x,y)$ is the solution of the adjoint boundary-value problem (B-6)-(B-7).

We express the gradient of the functional explicitly through the solution to the forward problem (1)-(2) and the adjoint problem (B-6)-(B-7). Therefore, at each step of a gradient descent method, we need to compute the solutions to the forward and adjoint problems only once regardless of on how many parameters the objective functional depends. The adjoint boundary-value problem (B-6)-(B-7) is of the same type as the forward problem (1)-(2). Hence, we can apply the support-operators method to discretize (B-6)-(B-7) in the same way as it has been done for problem (1)-(2). Moreover, the obtained formula for the gradient in Eq. (12) is exact: the only sources of error are numerical solutions of the boundary-value problems and numerical integration. If we tried to estimate the gradient via numerical differentiation, then we would inevitably introduce additional errors. In addition, numerical differentiation approach may require solving forward problem (1)-(2), many times depending on the number of identification parameters.

Note that the gradient of the functional in (12) is expressed through ∇p and $\nabla\psi$. However, for computations we do not need to numerically differentiate functions $p(x,y)$ and $\psi(x,y)$. Indeed, while constructing a discretization of the forward problem (1)-(2) we derived matrix $\mathcal{F}$ approximating the flux operator $K\nabla p$. Hence, we can put

$$\nabla p \approx \mathcal{X}^{-1}\Phi\mathcal{F}u \quad \text{and} \quad \nabla\psi \approx \mathcal{X}^{-1}\Phi\mathcal{F}\eta \quad \text{....(13)}$$

Here u is the discretization of p as above, and η is the discretization of ψ.

As we mentioned earlier, our goal is to estimate the angle of orientation of the main axes of the permeability tensor K if the eigenvalues k_1 and k_2 are known. Changing orientation of a symmetric positive definite tensor by an angle θ is equivalent to an orthogonal transformation of this tensor by the rotation matrix

$$R(\theta) = \begin{pmatrix} \cos\theta & -\sin\theta \\ \sin\theta & \cos\theta \end{pmatrix} \quad \text{.....(14)}$$

Put

$$K(\theta) = R^*(\theta) K R(\theta) \quad \text{.....(15)}$$

where $K = \begin{matrix} k_1 & 0 \\ 0 & k_2 \end{matrix}$. Then

$$\delta K(\theta) = \frac{d}{d\theta}K(\theta)\delta\theta = \left(\frac{d}{d\theta}R^*(\theta)KR(\theta) + R^*(\theta)K\frac{d}{d\theta}R(\theta)\right)\delta\theta \quad (16)$$

and from (12)

$$\frac{\partial J}{\partial\theta} = \int_{\Omega} -\nabla\psi \cdot \left(\frac{d}{d\theta}R^*(\theta)KR(\theta) + R^*(\theta)K\frac{d}{d\theta}R(\theta)\right)\nabla p\ d\Omega \quad \text{.(17)}$$

In Appendix C, we derive the second order derivative of functional J with respect to θ:

$$\begin{aligned} \frac{\partial^2 J}{\partial q^2} = &-\int_{\Omega} \nabla y \cdot \left(\left(\frac{d^2}{dq^2}K\right)\nabla p\right) d\Omega + \\ &+\int_{\Omega} \nabla y_1 \cdot \left(\left(\frac{d}{dq}K\right)\nabla p\right) d\Omega + \\ &+\int_{\Omega} \nabla y_2 \cdot \left(\left(\frac{d}{dq}K\right)\nabla y\right) d\Omega \end{aligned} \quad \text{.....(18)}$$

In order to apply Eq. (18), we need to solve two coupled boundary-value problems (C-8)-(C-11): the pair of functions ψ_1, ψ_2 in (18) is the solution to (C-8)-(C-11).

Solving the identification problem

Clearly the identification problem formulated above cannot be solved analytically. A discretization based on the support-operators method has been discussed above regarding the forward problem. The adjoint system (B-6)-(B-7) derived in Appendix B is a Dirichlet boundary-value problem for Poisson's equation of the same type as the forward problem (1)-(2). Therefore, the same discretization procedure can be applied to solve (B-6)-(B-7). Since matrix $\mathcal{A}$ in Eq. (7) is symmetric and positive definite, an iterative method such as

conjugate gradients is very efficient. The problem of inversion of matrix $\Phi^* \mathcal{K}^{-1} B \Phi$ is not difficult because it is a five-diagonal symmetric positive definite matrix and the method of conjugate gradients is very efficient in this case as well.

In order to evaluate the goodness of fit of the forward problem solution we discretize functional (10). Since the numerically obtained solution u evaluates pressure p at the centroid of each cell, a natural discretization of the functional is provided by

$$J \approx \frac{1}{2} \sum_{i=1}^{N_x} \sum_{j=1}^{N_y} w_{ij} \left(u_{ij} - p_{*ij} \right)^2 \left| Cell_{ij} \right| \text{.....(19)}$$

Here w_{ij} and p_{*ij} are the values of the weight function w and the measured pressure p_* at the centroid of cell (i,j), and $|Cell_{ij}|$ is the area of the cell.

If we have only one observation point where the pressure is measured, the weight function w is identically zero everywhere but in cell (i_0,j_0) where the measurements are available. Hence all the terms in Eq. (19), with exception of the term with indices (i_0,j_0), vanish and minimization of functional (19) reduces to minimization of a single term $u_{i_0 j_0} - p_{*i_0 j_0}{}^2$.

The gradient of functional (10) requires calculation of the gradients of the forward problem solution p and of the adjoint problem solution ψ. Computation of these gradients via numerical differentiation is problematic if we have a non-rectangular grid. However, the support-operators method furnishes the flux operator $\mathcal{F}$, so instead of explicit numerical differentiation we just apply Eq. (13). Thus, the discrete version of the gradient is given by

$$\frac{\partial J}{\partial \theta} \approx \sum_{i=1}^{N_x} \sum_{j=1}^{N_y} \left(\mathcal{K}^{-1} \Phi \mathcal{F} \eta \right)_{ij} \left(\tilde{\mathcal{K}} \mathcal{K}^{-1} \Phi \mathcal{F} u \right)_{ij} \left| Cell_{ij} \right| \text{. .....(20)}$$

Here $\tilde{\mathcal{K}}$ denotes the matrix generated by the derivative of the permeability tensor

$$\frac{d}{d\theta} K(\theta) = \frac{d}{d\theta} R^*(\theta) K R(\theta) + R^*(\theta) K \frac{d}{d\theta} R(\theta) \text{. .....(21)}$$

Finally, the minimization algorithm can be organized in the following way: first, pick up an initial guess θ_0. Then for each next iteration, θ_{n+1} is derived from θ_n using an iterative descent method:

$$\theta_{n+1} = \theta_n - \varepsilon_n \sum_{i=1}^{N_x} \sum_{j=1}^{N_y} \left(\mathcal{K}^{-1} \Phi \mathcal{F} \eta \right)_{ij} \left(\tilde{\mathcal{K}} \mathcal{K}^{-1} \Phi \mathcal{F} u \right)_{ij} \left| Cell_{ij} \right| \text{.(22)}$$

In the examples below, we determine the coefficient ε_n and the criterion for stopping iterations by Armijo's rule[15]. Equation (22) is equivalent to Newton method if

$$\varepsilon_n = \left(\frac{\partial^2 J}{\partial \theta^2} \right)^{-1} \approx$$

$$\sum_{i=1}^{N_x} \sum_{j=1}^{N_y} \left[\left(\mathcal{K}^{-1} \Phi \mathcal{F} \eta_1 \right)_{ij} \left(\tilde{\tilde{\mathcal{K}}} \mathcal{K}^{-1} \Phi \mathcal{F} u \right)_{ij} + \left(\mathcal{K}^{-1} \Phi \mathcal{F} \eta_1 \right)_{ij} \left(\tilde{\mathcal{K}} \mathcal{K}^{-1} \Phi \mathcal{F} u \right)_{ij} \right.$$

$$\left. + \left(\mathcal{K}^{-1} \mathcal{F} \eta_2 \right)_{ij} \left(\tilde{\mathcal{K}} \mathcal{K}^{-1} \mathcal{F} \eta \right)_{ij} \right] \left| Cell_{ij} \right|^{-1} \text{,.....(23)}$$

where $\tilde{\tilde{\mathcal{K}}}$ denotes the matrix generated by the second derivative of the permeability tensor and η_1 and η_2 are the discrete versions of ψ_1 and ψ_2, respectively.

In the approach we have been developing so far, the adjoint system and the gradient are obtained first, and both the forward and the adjoint problems are discretized simultaneously. An alternative approach is to begin with discretization of the forward problem and the functional, and then to obtain the adjoint system and the gradient for an already discretized forward problem. In such a way, we do not derive the differential adjoint equation, but immediately obtain a discrete system. In Appendix D, we derive all the relevant equations. Normally derivation of the adjoint system to already discretized equations leads to severe difficulties because calculations involve multiple indices and are quite cumbersome. The framework of the support-operators method simplifies these calculations significantly.

Similarly to Appendix C, we can derive the discrete second adjoint equations and obtain the second derivative of functional (19). However, we do not present these results here.

There is no obvious preference to which method is better: the adjoint system first and discretization after that, or vice versa, first the discretization and then the adjoint system. Error in estimating the gradient by the first approach originates from the numerical solution of the forward and adjoint boundary-value problems and from truncation errors in evaluating the gradient, Eq. (20). The second approach provides the gradient of the functional only subject to round-off computational errors. However, from the beginning we solve not the original problem, but its discrete approximation. In test examples, we observed no dramatic difference in the results produced by the two methods.

Example. In order to illustrate the method developed above consider the following example. To generate the target solution, we solve a forward problem (1)-(2) with zero boundary condition and permeability tensor $K_* = \begin{matrix} 7.75 & 3.8971 \\ 3.8971 & 3.25 \end{matrix}$ that corresponds to a rotation of the

diagonal tensor $\begin{matrix} 10 & 0 \\ 0 & 1 \end{matrix}$ by the angle $\pi / 6$. We take the source function *f* and the weight function *w* as approximations to Dirac's delta function concentrated at one point. Assuming various initial guesses about the rotation angle θ, we applied the gradient descent method with Armijo's rule of selecting the gradient step ε and the criterion for stopping iterations. The algorithm is realized in Matlab[16], so we do not need to bother about inverting matrices or solving systems of linear equations. On a rectangular grid, the initial value of the functional 1.9343 has been reduced to 3.6e-007 and the angle of rotation has been found with absolute error of 1.3e-004. Tensor K_* has been identified with absolute error of 1e-3. The results of application of the algorithm on two curvilinear grids are presented in **Fig. 8** - **Fig. 10** and in Table 1. The number of iterations and the elapsed time of computations depend on the grid. Curvilinear grid takes more time because the flux matrix is full. The number of iterations of descent method depends on how "lucky" we are with the initial guess. Clearly, functional (10) and its discrete approximation (19) are periodic functions of θ. If the initial guess is close to the maximum of (10), then the first iterations move slowly towards the minimum, because the gradient is close to zero. Then the iterations accelerate and we observed the geometric convergence. In all the examples presented here, the initial guess was "bad enough": $\theta_0 = -\pi / 6$. In Fig. 8-Fig. 10, the top left plot is the graph of the target solution. The left bottom plot is the graph of the initial guess. In the right top plot, we graph the solution of the adjoint boundary-value problem. As we can observe, $\psi(x, y)$ is almost equal to zero everywhere outside a small neighborhood of the point where the target solution is evaluated and where the weight function *w* is not equal to zero. The right bottom plot is the graph of the solution obtained for the recovered value of θ. Close similarity to the plot of the target function needs no comment.

Conclusions

- A finite difference scheme of finding the orientation of permeability tensor in an anisotropic porous medium has been proposed.
- The scheme is based on the method of support operators and is coordinate independent, allowing computation of a solution in cases where the permeability tensor is highly anisotropic and the grid is curvilinear.
- A problem of identification of orientation of anisotropic permeability tensor has been formulated. The first and second differentials of the performance criterion have been obtained via adjoint system approach.
- The numerical method of solving forward boundary-value problem can be equally applied to solving the adjoint problems of first and second order.
- The gradient and adjoint system have been derived for the discretized formulations of the forward problem as well.
- A minimization algorithm based on the formulae for the gradient and discretization via support-operators method has been developed. The algorithm has been verified on several synthetic examples involving computations on rectangular and curvilinear grids. The algorithm demonstrated good convergence to the minimum and the searched angle of orientation of the permeability tensor is estimated with good precision. The algorithm has been implemented in Matlab.

Nomenclature

B Matrix of cubature coefficients
$|Cell_{ij}|$ Volume of the cell (i,j)
DIV Matrix of discretized divergence operator
J Performance criterion
K Permeability tensor
N_x, N_y Dimensions of the grid
R Matrix of rotation
f Density of sources
i, j, ν Dummy indices
p Pressure
p_* Measured pressure
u Discretized pressure
w Weight function
$\mathcal{A}$ The matrix of coefficients of discretized equations
$\mathcal{F}$ The matrix of discretized flux operator
$\mathcal{K}^{-1}$ Matrix derived from the inverse permeability tensor
Γ Boundary of the domain on which the equations are being solved
Λ Diagonal matrix with the volumes of the grid cells on the main diagonal
Ω, Ω_h Domain and discretized domain on which the equations are being solved
ε_n Step size in gradient descent method
θ Angle of orientation of the permeability tensor
ψ, ψ_1, ψ_2 Solutions of first and second adjoint problems

Acknowledgements

This work was supported in part by two members of the U.C. Oil® Consortium, Chevron USA and Aera Energy. Partial support was also provided by the Assistant Secretary for Fossil Energy, Office of Gas and Petroleum Technology, under contract No. DE-ACO3-76FS00098 to the Lawrence Berkeley National Laboratory of the University of California.

References

1.Elkins, L.F., "Reservoir Performance and Well Spacing - Silica Arbuckle Pool,". *Drill. and Prod. Prac., API*, 1946: p. 109.

2.Elkins, L.F., Skov, A.M., "Determination of Fracture Orientation from Pressure Interference,". *Journal of Petroleum Technology*, 1960(December): p. 301-304.
3.Romm, E.S., *Permeability properties of fissured rock (in Russian)*. 1966, Moscow: Nedra.
4.Ramey, H.J., "Interference Analysis for Anisotropic Formations - A case History". *Journal of Petroleum Technology*, 1975(October): p. 1290-1298.
5.Guo, B., Schechter, D.S., Banik, A. *Use of Single-Well Test Data for Estimating Permeability Anisotropy of the Naturally Fractured Spraberry Trend Area Reservoirs, SPE 39807*. in *Permian Basin Oil and Gas Recovery Conference*. 1998. Midland, Texas: SPE.
6.Da Prat, G., *Well Test Analysis for Fracture Reservoir Evaluation*. 1990, N.Y.: Elsevier Scince Publishing Co.
7.Muskat, M., *The Flow of Homogeneous Fluids through Porous Media*. 1946, Ann Arbor, MI: J.W.Edwards, Inc.
8.Shashkov, M., *Conservative Finite-Difference Methods on General Grids*. 1995, Boca Raton, FL: CRC Press.
9.Shashkov, M., Steinberg, S., "Solving Diffusion Equations with Rough Coefficients in Rough Grids,". *Journal of Computational Physics*, 1996. **129**: p. 383-405.
10.Tikhonov, A.N., and Samarskii, A. A., *Equations of mathematical physics*. International series of monographs in pure and applied mathematics; v. 39. 1963, New York: Macmillan.
11.Carslaw, J.C., and Jaeger, J. C., *Conduction of Heat in Solids*. 2 ed. 1959: Clarendon Press, Oxford.
12.Narasimhan, T.N., Witherspoon, P.A., "An Integrated Finite Difference Method for Analyzing Fluid Flow in Porous Media,". *Water Resources Research*, 1976. **12**(1): p. 57-64.
13.Edwards, M.G., Rogers, C.F., "Finite Volume Discretization with Imposed Flux Continuity for the General Tensor Pressure Equation,". *Computational Geosciences*, 1998. **2**: p. 259-290.
14.Edwards, M.G. *Split Elliptic Tensor Operators for Reservoir Simulation*. in *ICFD Conference on Numerical Methods for Fluid Dynamics*. 1998. Oxford, UK: Oxford University.
15.Bertsekas, D.P., *Constrained optimization and Lagrange multiplier methods*. 1982, N.Y.: Academic Press.
16."Matlab. The Language of Technical Computing," 1998, The MathWorks, Inc.
17.Hildebrand, F.B., *Introduction to Numerical Analysis*. 1956, N.Y.: McGraw-Hill.
18.Vasil'ev, F.P., *Numerical Methods for Solving Extremal Problems (in Russian)*. 1982, Moscow: Nauka.

Appendix A. Discretization of Gauss-Ostrogradski divergence theorem

In this appendix, we outline the main constructions of the method of support-operators we use to identify anisotropy of permeability tensor. The theory of the method is explained in more detail in Ref.[8].

First, let us recall the Gauss-Ostrogradski divergence theorem: given a vector field w and a scalar function u defined over a domain Ω with the boundary $\Gamma = \partial\Omega$, the following equality holds true:

$$\int_\Omega u\nabla\cdot w d\Omega + \int_\Omega \nabla u\cdot w d\Omega = \oint_\Gamma uw\cdot n d\Gamma \ ,.....(A\text{-}1)$$

where n is the outer normal at the surface Γ. We assume that both the vector field w and function u are smooth enough and that the domain Ω has sufficiently regular boundary. Here we need a slight modification of (A-1). If K is a symmetric positive definite tensor defined on $\Omega\cup\Gamma$, then

$$\int_\Omega K\nabla u\cdot K^{-1}w d\Omega = \oint_\Gamma uw\cdot n d\Gamma - \int_\Omega u\nabla\cdot w d\Omega \ .....(A\text{-}2)$$

Equation (A-2) can be interpreted as the definition of the flux operator $K\nabla u$. Indeed, if we pick up a smooth function u defined over $\Omega\cup\Gamma$, then there exists only one vector field U such that

$$\int_\Omega U\cdot K^{-1}w d\Omega = \oint_\Gamma uw\cdot n d\Gamma - \int_\Omega u\nabla\cdot w d\Omega \ .....(A\text{-}3)$$

holds true for an arbitrary vector field w. From (A-2) $U = K\nabla u$. Therefore, the definition of the flux operator is given through the divergence operator. In a sense, the flux operator is "supported" by divergence. This property is fundamental to the discretization by the method of support operators.

Theoretically, Eq. (A-3) can be "reversed." The divergence can be defined through the flux operator, i.e., the divergence and flux are dual to each other. Practically, it is more natural to use (A-2)-(A-3) to define flux through divergence, than vice versa.

In order to use definition (A-3) to discretize Eq. (1) we need the following steps. First, we discretize the divergence. Then, using this discretization, we discretize Eq. (A-3). The third step is to resolve Eq. (A-3) with respect to U. Since the right-hand side is linear with respect to u, we will treat U as a linear transformation of u, which reduces to a matrix in the discretized equation. After all these steps are completed, it only remains to take superposition of the discretized divergence and flux in order to obtain a discretization of the boundary-value problem (1)-(2).

Discretization of divergence. Assume that we have a 2D grid Ω_h with quadrilateral cells. Consider a cell with indices (i, j), $1 \le i \le N_x$, $1 \le j \le N_y$. Denote by $f_{ij}^{1,2,3,4}$ the fluxes through the four boundaries of the cell. We assume the positive directions to be north and east, i.e., $f_{ij}^{1,4}$ are fluxes along the inner normals, and $f_{ij}^{2,3}$ are fluxes along the outer normals, Fig. 2. Each f_{ij}^{ν}, ν=1,2,3,4, is a scalar. Remark that f is the normal component of the flux and it is continuous across the boundary of the cell even for heterogeneous and anisotropic medium. The flux vector is evaluated at the vertices of the cell and we denote its values by $w_{ij}^{1,2,3,4}$, Fig. 2. Clearly, the projections of vectors $w_{ij}^{1,2,3,4}$ on the respective

outer unit normals, $n_{ij}^{1,2,3,4}$, should yield $f_{ij}^{1,2,3,4}$ with appropriate signs. Hence, there is a linear transformation mapping the array of all flux vectors $w_{ij}^{1,2,3,4}$ evaluated in every grid cell to the array of all f_{ij}^{ν}. This transformation can be obtained through cumbersome but straightforward calculations. Moreover, it can be seen that there also exists an inverse transformation of the array of all $f_{ij}^{1,2,3,4}$ into array $w_{ij}^{1,2,3,4}$, and this inverse transformation can be explicitly calculated too. Omitting details, let us denote the array of all $f_{ij}^{1,2,3,4}$ by *f*, the array of all $w_{ij}^{1,2,3,4}$ by *w*, and the transformation mapping *f* into *w* by Φ:

$$w = \Phi f \quad \text{.....(A-4)}$$

The structure of matrix Φ is determined by the structure of grid Ω_h only and there is no dependence on *w* or *f*.

To construct our discretization of Eq. (1), we begin with discretizing divergence in each cell. By definition

$$\nabla \cdot w = \lim_{|V|\to 0} \frac{1}{|V|} \oint_{\partial V} \langle w, n \rangle ds \quad \text{.....(A-5)}$$

Here $|V|$ denotes the volume of domain *V* which contracts to a point as we pass to the limit; *n* is the outer unit normal to *V* at its boundary ∂V at a surface element *ds*. If we replace the limit in Eq. (A-5) by the same expression evaluated on a finite domain *V*, we obtain a discrete approximation of divergence. It is not difficult to show that this approximation is of second order with respect to the size of domain *V* when divergence is evaluated at the centroid of *V*. In the 2D case, we can take our cell as a finite small domain for the computation of the approximate divergence:

$$(DIVw)_{ij} \approx \frac{1}{|Cell_{ij}|} \sum_{\nu=1}^{4} f_{ij}^{\nu} l_{ij}^{\nu} \quad \text{.....(A-6)}$$

where l_{ij}^{ν} are the lengths of the sides of $Cell_{ij}$, $|Cell_{ij}|$ is the volume of $Cell_{ij}$. As in Ref.[8], we formally extend *DIV* to the boundary of Ω_h by putting $(DIVw)_{ij} = -f_{ij}^{\nu}$, where ν is the index of the cell edge along the boundary of Ω_h, **Fig. 6.** In the case of the Dirichlet boundary condition, this extension is not important and it is done here only for consistency with Ref.[8].

Discretization of the integrals in Equation (A-2)**.** Equation (A-2) involves two kinds of integrals: two integrals over the domain, Ω, and one surface integral over $\Gamma = \partial\Omega$. Since in our case the boundary of the discretized domain Ω_h is given by a closed polygonal line, for the surface integral we apply the quadrature rule of rectangles with the integrand evaluated at the midpoint[17]:

$$\oint_{\Gamma} uw \cdot nd\Gamma \approx \sum_{j=1}^{N_y} u_{1/2\,j} f_{1\,j}^{1} l_{1\,j}^{1} + u_{N_x+1/2\;\;j} f_{N_x\,j}^{3} l_{N_x\,j}^{3}$$

$$+ \sum_{i=1}^{N_x} u_{i\,1/2} f_{i1}^{4} l_{i1}^{4} + u_{i\;N_y+1/2} f_{i\;N_y}^{2} l_{i\;N_y}^{2} \quad \text{.....(A-7)}$$

The integral $\int_{\Omega} u\nabla \cdot wd\Omega$ can be discretized straightforwardly, because the integrand is evaluated at the centroid of each cell:

$$\int_{\Omega} u\nabla \cdot wd\Omega \approx \sum_{i=1}^{N_x} \sum_{j=1}^{N_y} u_{ij}\ DIV\ f_{ij} |Cell_{ij}| = \Lambda u \cdot DIV\ f, \quad \text{(A-8)}$$

where Λ is a diagonal matrix whose elements are equal to $|Cell_{ij}|$. In particular, matrix Λ is positive definite.

Substitution of Eq. (A-6) into Eq. (A-8) yields

$$\int_{\Omega} u\nabla \cdot wd\Omega \approx \sum_{i=1}^{N_x} \sum_{j=1}^{N_y} u_{ij} \sum_{\nu=1}^{4} f_{ij}^{\nu} l_{ij}^{\nu} \quad \text{.....(A-9)}$$

where coefficients l_{ij}^{ν} are defined above, see Eq. (A-6).

Now let us discretize the second integral on the left-hand side of Eq. (A-2). For this purpose, consider an auxiliary integral

$$I = \int_{\Omega} v \cdot K^{-1} wd\Omega \quad \text{.....(A-10)}$$

where *v* and *w* are two vector fields defined on $\Omega \cup \Gamma$ and *K* is the positive definite permeability tensor from Eq. (1). Numerical integration of the scalar product of two vector fields reduces to the problem of numerical integration of a scalar function, which is evaluated at the vertices of the cells. At each vertex, however, the function may take up to four different values affiliated with neighboring cells for which the vertex is common. Consequently, we calculate the integral over each individual cell and then sum up over all cells.

Denote the values affiliated with $Cell_{ij}$ by $z_{ij}^{1,2,3,4}$:

$$z_{ij}^{\nu} = v_{ij}^{\nu} \cdot K^{-1} w_{ij}^{\nu}, \qquad \nu = 1,2,3,4 \quad \text{.....(A-11)}$$

see **Fig. 7**. Denote by $\beta_{ij}^{1,2,3,4}$ the cubature coefficients for the numerical integration over cell (*i*,*j*). The integral of the discrete function z over the cell is then given by

$$I_{ij} = \sum_{\nu=1}^{4} \beta_{ij}^{\nu} z_{ij}^{\nu} \quad \text{.....(A-12)}$$

There are different ways of defining the coefficients $\beta_{ij}^{1,2,3,4}$. In the examples below, $\beta_{ij}^{1,2,3,4}$ were defined in such a way that Eq. (A-12) provided exact evaluation of integrals of a constant, of a linear function and of the product *xy*. Hence, at each cell the coefficients $\beta_{ij}^{1,2,3,4}$ are found from solution to a system of four linear equations.

Summing up over all indices *i, j*, we obtain

$$I \approx \sum_{i=1}^{N_x}\sum_{j=1}^{N_y}\sum_{\nu=1}^{4}\beta_{ij}^{\nu}v_{ij}^{\nu}\cdot K^{-1}w_{ij}^{\nu} \quad \text{.....(A-13)}$$

It is possible to prove that if the cubature coefficients $\beta_{ij}^{1,2,3,4}$ are selected as described above, then error in Eq. (A-13) is of second order with respect to the greatest diameter of the cells. The iterated sum on the right-hand side of Eq. (A-13) is a bilinear form with respect to *v* and *w*. Let us write it down in matrix notation:

$$\sum_{i=1}^{N_x}\sum_{j=1}^{N_y}\sum_{\nu=1}^{4}\beta_{ij}^{\nu}v_{ij}^{\nu}\cdot K^{-1}w_{ij}^{\nu} = Bv\cdot\mathcal{K}^{-1}w \quad \text{.....(A-14)}$$

where *B* is the diagonal matrix of coefficients $\beta_{ij}^{1,2,3,4}$ and $\mathcal{K}^{-1}$ is the matrix derived from the inverse tensor K^{-1}. Clearly, $\mathcal{K}^{-1}$ is symmetric and positive definite. Let us assume that every cell of grid Ω_h is convex, then from Eq. (A-14) matrix $\mathcal{K}^{-1}B$ is symmetric and positive definite as well.

Now denote by $\mathcal{F}$ the matrix discretizing the flux operator:

$$K\nabla p \approx \mathcal{F}u \quad \text{.....(A-15)}$$

where *u* is the array of the values of pressure at the centroid of each cell. On the boundaries of each cell matrix $\mathcal{F}$ maps *u* into an array of normal fluxes. Combining Eqs. (A-4), (A-10), (A-13), (A-14) and (A-15) together, we obtain

$$\int_{\Omega} K\nabla p\cdot K^{-1}w\,d\Omega \approx \Phi\mathcal{F}u\cdot\mathcal{K}^{-1}B\Phi f \quad \text{.....(A-16)}$$

Finally, the discretization of the Gauss-Ostrogradski divergence theorem yields the following equation

$$\mathcal{F}u\cdot\Phi^{*}\mathcal{K}^{-1}B\Phi f = -\Lambda u\cdot DIV\ f$$

$$+\sum_{j=1}^{N_y} u_{1/2\ j}f_{1j}^{1}l_{1j}^{1} + u_{N_x+1/2\ j}f_{N_x j}^{3}l_{N_x j}^{3} \quad \text{.....(A-17)}$$

$$+\sum_{j=1}^{N_y} u_{i1/2}f_{i1}^{4}l_{i1}^{4} + u_{i\,N_y+1/2}f_{iN_y}^{2}l_{iN_y}^{2} \quad .$$

Appendix B. Gradient of functional (10) via adjoint system

Let us derive the adjoint system for the problem of minimization of functional (10) subject to the constraint specified by the boundary-value problem (1)-(2). This is a standard method of deriving the gradient in a constrained optimization problem[18]. Assume a small perturbation δK of the permeability tensor *K* such that $K+\delta K$ also is a symmetric positive tensor. Then put $J[K]+\delta J = J[K+\delta K]$ and denote by $p+\delta p$ the solution to the boundary-value problem

$$\nabla\cdot\big((K+\delta K)\nabla(p+\delta p)\big) = -f\ ,\ (x,y)\in\Omega\ ,\quad (1_\delta)$$

$$(p+\delta p)\big|_{\Gamma} = \phi\ . \quad (2_\delta)$$

Neglecting the terms of order higher than one, we obtain

$$\delta J = \int_{\Omega} w(x,y)\ \ p(x,y) - p_{*}(x,y)\ \ \delta p(x,y)\,d\Omega\ , \quad \text{.....(B-1)}$$

where δp satisfies the boundary-value problem in variations

$$\nabla\cdot(\delta K\nabla p) + \nabla\cdot(K\nabla(\delta p)) = 0\ ,\quad x,y\ \in\Omega\ , \quad \text{.....(B-2)}$$

$$\delta p\big|_{\Gamma} = 0\ . \quad \text{.....(B-3)}$$

Multiply Eq. (B-2) by an adjoint variable $\psi(x,y)$, integrate over Ω and add to Eq. (B-1). Then

$$\delta J = \int_{\Omega} w(x,y)\ \ p(x,y) - p_{*}(x,y)\ \ \delta p(x,y)\,d\Omega + \quad \text{.....(B-4)}$$

$$\int_{\Omega} \psi\nabla\cdot(\delta K\nabla p) + \psi\nabla\cdot(K\nabla(\delta p))\,d\Omega\ .$$

Using the Gauss-Ostrogradski divergence theorem and taking into account Eq. (B-3), we obtain

$$\int_{\Omega} \psi\nabla\cdot(\delta K\nabla p) + \psi\nabla\cdot\big(K\nabla(\delta p)\big)\,d\Omega =$$

$$\int_{\Omega} -\nabla\psi\cdot(\delta K\nabla p) + \delta p\nabla\cdot(K\nabla\psi)\,d\Omega + \quad \text{....(B-5)}$$

$$\int_{\Gamma} \psi(\delta K\nabla p + K\delta p)\cdot n\,d\Gamma\ .$$

Now, if $\psi(x,y)$ solves the adjoint boundary-value problem

$$\nabla\cdot(K\nabla\psi) = -w(x,y)\ \ p(x,y) - p_{*}(x,y)\ \ , \quad \text{.....(B-6)}$$

$$\psi\big|_{\Gamma} = 0\ , \quad \text{.....(B-7)}$$

then, from (B-4)-(B-5), the variation of functional (10) is equal to

$$\delta J = \int_{\Omega} -\nabla\psi \cdot (\delta K \nabla p) d\Omega \quad \text{.....(B-8)}$$

Appendix C. Differential of second order via second adjoint system

The analysis presented in Appendix B can be extended to calculating the second differential of functional (10). In this appendix, we derive the second adjoint system of equations and express the second order derivative of Eq. (10) through the solution of the second adjoint system. In a general case, the second order differential is a quadratic form over a functional space[18] and the calculations can be rather complicated. It is easier to calculate a directional derivative, rather than the Hessian. However, in our particular situation there is only one parameter of optimization. Consequently, the calculations can be fully accomplished and we derive a pair of coupled boundary-value problems of the same type as Eqs. (1)-(2).

Since the second derivative is the derivative of the first derivative, we can calculate $\frac{\partial^2}{\partial\theta^2} J(\theta)$ in a similar way as we obtained Eq. (17). Indeed, in order to calculate Eq. (17) we solve a pair of boundary-value problems (1)-(2) and (B-6)-(B-7). Therefore, we can interpret Eq. (17) as another functional and Eqs. (1)-(2), (B-6)-(B-7) as a system of constraints. Then, assuming a small variation $\delta\theta$ of θ, we obtain

$$\delta g(\theta) = \int_{\Omega} -\nabla\delta\psi \cdot \left(\frac{d}{d\theta} K(\theta) \nabla p \right) d\Omega +$$

$$\int_{\Omega} -\nabla\psi \cdot \left(\left(\frac{d^2}{d\theta^2} K(\theta) \right) \nabla p \right) d\Omega \delta\theta + \int_{\Omega} -\nabla\delta\psi \cdot \left(\left(\frac{d}{d\theta} K(\theta) \right) \nabla\delta p \right) d\Omega \quad \text{.....(C-1)}$$

where $g(\theta) = \frac{\partial J(\theta)}{\partial\theta}$. Similarly to Eqs. (B-2) - (B-3) in Appendix B, we obtain the following tangent boundary-value problems for variations δp and $\delta\psi$:

$$\nabla \cdot \left(\frac{d}{d\theta} K \nabla p \right) \delta\theta + \nabla \cdot \left(K \nabla (\delta p) \right) = 0, \quad x, y \in \Omega \quad \text{..(C-2)}$$

$$\delta p\big|_{\Gamma} = 0 \quad \text{.....(C-3)}$$

and

$$\nabla \cdot \left(\frac{d}{d\theta} K \nabla\psi \right) \delta\theta + \nabla \cdot \left(K \nabla (\delta\psi) \right) + w\delta p = 0, \quad x, y \in \Omega \quad \text{.(C-4)}$$

$$\delta\psi\big|_{\Gamma} = 0 \quad \text{.....(C-5)}$$

Now let us introduce two auxiliary adjoint variables $\psi_1(x, y)$ and $\psi_2(x, y)$. Multiply (C-2) and (C-4) by $\psi_1(x, y)$ and $\psi_2(x, y)$, respectively, integrate the result over Ω and add to (C-1). Straightforward calculations involving several iterations of the Gauss-Ostrogradski divergence theorem yield

$$\delta g(\theta) =$$

$$\int_{\Omega} -\nabla y \cdot \left(\left(\frac{d^2}{dq^2} K(q) \right) \nabla p \right) d\Omega dq +$$

$$\int_{\Omega} +\nabla y_1 \cdot \left(\frac{d}{dq} K \nabla p \right) d\Omega dq +$$

$$\int_{\Omega} -\nabla y_2 \cdot \left(\frac{d}{dq} K \nabla y \right) d\Omega dq$$

$$+ \int_{\Omega} \delta p \left(\nabla \cdot \left(K(\theta) \nabla\psi_1 \right) - \nabla \cdot \left(\left(\frac{d}{d\theta} K(\theta) \right) \nabla\psi \right) + w\psi_2 \right) d\Omega$$

$$+ \int_{\Omega} \delta\psi \left(\nabla \cdot \left(K(\theta) \nabla\psi_2 \right) - \nabla \cdot \left(\frac{d}{d\theta} K(\theta) \nabla p \right) \right) d\Omega \quad \text{....(C-6)}$$

$$+ \int_{\Gamma} \psi_1 \nabla \cdot (K(\theta) \nabla\delta p) d\Gamma + \int_{\Gamma} \psi_2 \nabla \cdot (K(\theta) \nabla\delta\psi) d\Gamma .$$

Finally, we obtain that

$$\frac{\partial^2 J}{\partial\theta^2} = -\int_{\Omega} \nabla\psi \cdot \left(\left(\frac{d^2}{d\theta^2} K \right) \nabla p \right) + \nabla\psi_1 \cdot \left(\left(\frac{d}{d\theta} K \right) \nabla p \right) + \nabla\psi_2 \cdot \left(\left(\frac{d}{d\theta} K \right) \nabla\psi \right) d\Omega \quad \text{(C-7)}$$

where p is the solution to the forward problem (1)-(2), ψ is the solution to the first adjoint problem (B-2)-(B-3), and ψ_1, ψ_2 are, respectively, the solutions to the following pair of boundary value problems:

$$\nabla \cdot \left(K(\theta) \nabla\psi_1 \right) = \nabla \cdot \left(\frac{d}{d\theta} K(\theta) \nabla\psi \right) - w\psi_2 \quad \text{.....(C-8)}$$

$$\psi_1\big|_{\Gamma} = 0 \quad \text{.....(C-9)}$$

$$\nabla \cdot \left(K(\theta) \nabla\psi_2 \right) = \nabla \cdot \left(\frac{d}{d\theta} K(\theta) \nabla p \right) \quad \text{.....(C-10)}$$

$$\psi_2\big|_{\Gamma} = 0 \quad \text{.....(C-11)}$$

which yield the second adjoint system . Note that Eqs. (1), (C-4), (C-8) and (C-10) are replicas of the same elliptic equation with different right-hand sides. The same holds true with regard to the boundary conditions. Therefore, the same

discretization and solution routines can be used for all of them.

Summing up, in order to find the second derivative of functional (10), we first we solve the forward problem (1)-(2); second, we solve the first adjoint problem (B-2)-(B-3); and third we solve the boundary problems (C-8)-(C-11).

Second order derivatives are used in Newton's descent method, which is very efficient in minimization. In many cases, given a good initial guess, Newton's method provides convergence to the solution in a few iterations[18]. However, there is an overhead of solving four boundary-value problems per iteration. Moreover, as the number of optimization parameters increases, the number of boundary-value problems solved to calculate the second differential of the functional increases as well.

Appendix D. Discrete version of adjoint system and the gradient

In Appendix B, we have derived the adjoint system for calculating the gradient of functional (10) subject to constraints (1)-(2). In effect, the forward and adjoint problems have been discretized independently of each other. This circumstance does not cause any problems in our particular case since our discretization produces a symmetric positive definite matrix. In a general case, however, discretization of the adjoint problem depends on discretization of the forward problem. These discretizations will be coupled if we first discretize the forward problem and then derive the adjoint system in discretized form. The latter approach usually leads to cumbersome calculations since the discrete system of equations has multiple indices. A software package admitting symbolic computations could be useful to avoid errors.

The support-operators method allows us to reduce the burden of calculations because of a clear matrix representation (7)-(9) of the discrete equations. In this appendix, we obtain the system of equations adjoint to (7).

Note that in Eqs. (7)-(9) only matrix $\mathcal{A}$ depends on the optimization parameter θ. Therefore, if θ is perturbed by a small variation $\delta\theta$, then the equation in variations is

$$\delta\mathcal{A}u + \mathcal{A}\delta u = \delta\mathbf{b} \quad \text{.....(D-1)}$$

The variation of functional (19) is equal to

$$\delta J = \sum_{i=1}^{N_x}\sum_{j=1}^{N_y} w_{ij}\ u_{ij} - p_{*ij}\ \delta u_{ij}\left|Cell_{ij}\right| \quad \text{.....(D-2)}$$

Let us introduce the adjoint discrete variable ψ_{ij}. Multiply Eq. (D-1) by $\psi_{ij}\left|Cell_{ij}\right|$ element by element and add the sum over all i,j to Eq. (D-2). We obtain

$$\delta J = \sum_{i=1}^{N_x}\sum_{j=1}^{N_y} w_{ij}\ u_{ij} - p_{*ij}\ + (\mathcal{A}\psi)_{ij}\ \left|Cell_{ij}\right|\delta u_{ij} +$$

$$\sum_{i=1}^{N_x}\sum_{j=1}^{N_y} (\delta\mathcal{A})^{*}\psi_{\ ij} - \delta\mathbf{b}_{ij}\psi_{ij}\ \left|Cell_{ij}\right| \quad \text{....(D-3)}$$

Because of Eqs. (8), (9), to calculate $\delta\mathcal{A}$ and $\delta\mathbf{b}$ we also need to calculate the variation of matrix $\Phi^{*}\mathcal{K}^{-1}B\Phi^{\ -1}$. Clearly,

$$\delta\ \Phi^{*}\mathcal{K}^{-1}B\Phi^{\ -1} = \text{.....(D-4)}$$

$$\Phi^{*}\mathcal{K}^{-1}B\Phi^{\ -1}\Phi^{*}\frac{d}{d\theta}\mathcal{K}^{-1}B\Phi\ \Phi^{*}\mathcal{K}^{-1}B\Phi^{\ -1}\delta\theta\,.$$

Further, $\mathcal{K}^{-1}$ depends linearly on $K(\theta)^{-1}$, see Eq. (A-14) in Appendix A. Hence

$$\frac{d}{d\theta}\mathcal{K}^{-1}\ K(\theta)^{-1}\ = \mathcal{K}^{-1}\ \frac{d}{d\theta}K(\theta)^{-1}\quad \text{,.....(D-5)}$$

where

$$\frac{d}{d\theta}K(\theta)^{-1} = K(\theta)^{-1}\frac{d}{d\theta}K(\theta)K(\theta)^{-1} \quad \text{.....(D-6)}$$

and for $\frac{d}{d\theta}K(\theta)$ we already have formula (16).

Thus, from Eqs. (D-2)-(D-4), we finally obtain

$$\frac{\partial J}{\partial\theta} = \sum_{i=1}^{N_x}\sum_{j=1}^{N_y}\left(\left(\left(\Lambda DIV\left(\Phi^{*}\mathcal{K}^{-1}B\Phi\right)^{-1}\Phi^{*}\frac{d}{d\theta}\mathcal{K}^{-1}B\Phi\mathcal{F}\right)^{*}\psi\right)_{ij} -\right.$$

$$\left.+\left(\left(\Phi^{*}\mathcal{K}^{-1}B\Phi\right)^{-1}\Phi^{*}\frac{d}{d\theta}\mathcal{K}^{-1}B\Phi\left(\Phi^{*}\mathcal{K}^{-1}B\Phi\right)^{-1}\Lambda_b u_b\right)_{ij}\psi_{ij}\right)\left|Cell_{ij}\right| \quad \text{(D-7)}$$

where $\frac{d}{d\theta}\mathcal{K}^{-1}$ is calculated through Eqs. (D-5)-(D-6).

TABLE 1--RESULTS OF COMPUTATIONS

Figure	Initial value of the functional	Final value of the functional	Absolute error of angle estimation
Fig. 8	1.9343	3.6e-007	1.3e-004
Fig. 9	2.3514	5.0e-006	4.5e-004
Fig. 10	1.5057	3.04e-007	1.3e-004

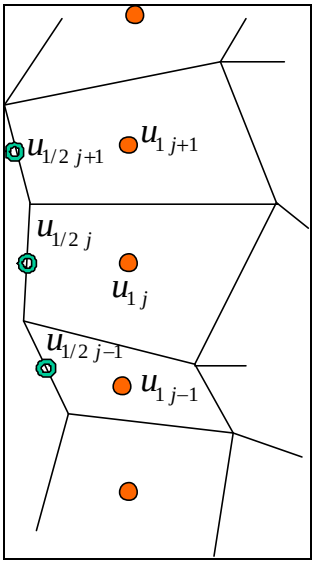

Fig. 1 - Indexing of the interior and boundary cells.

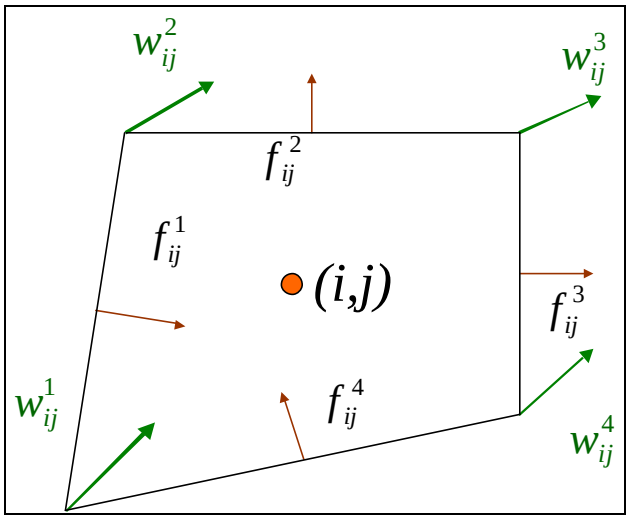

Fig. 2 - *Cell(i,j)*: $f_{ij}^{1,2,3,4}$ are the normal components of the fluxes attached to the walls of the cell, $w_{ij}^{1,2,3,4}$ are the fluxes at the corners of the cell.

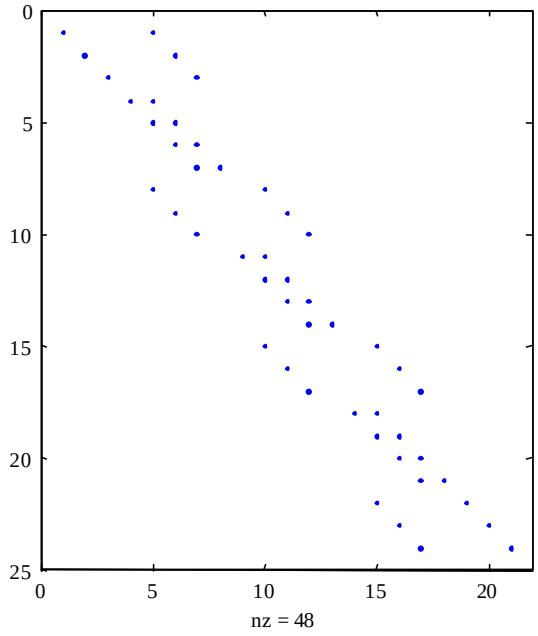

Fig. 3 - The structure of the flux operator matrix on a rectangular grid.

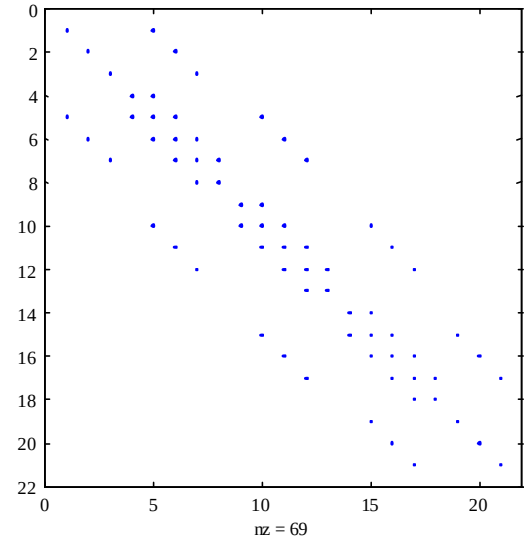

Fig. 4 - The structure of discretized Laplace operator $\nabla \cdot K \nabla p$ on a rectangular grid.

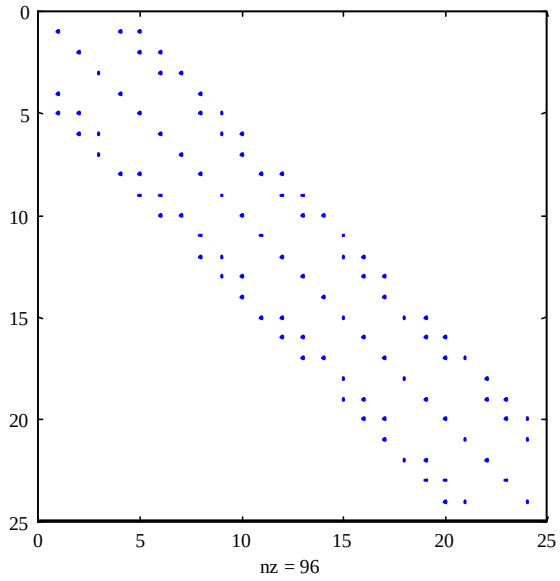

Fig. 5 - The structure of the matrix $\Phi^{*}K^{-1}B\Phi$ on an irregular grid.

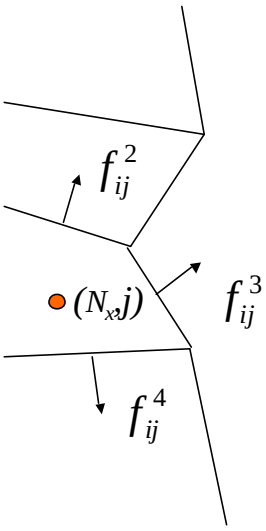

Fig. 6 - Formal extension of DIV to the boundary: $(\mathrm{DIV}\, w)_{N_x+1/2\, j} = f^{3}_{N_x j}$.

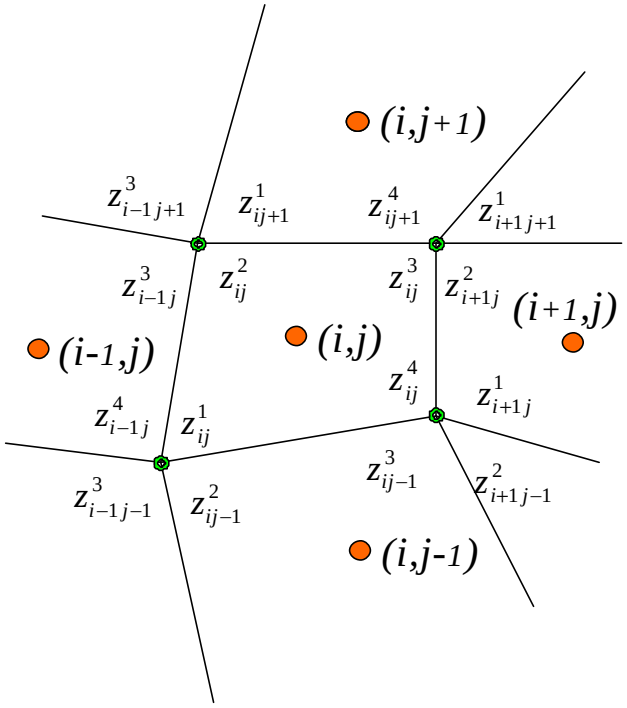

Fig. 7 - The scalar function *z* may take up to four different values at each vertex of the *Cell(j,j).*

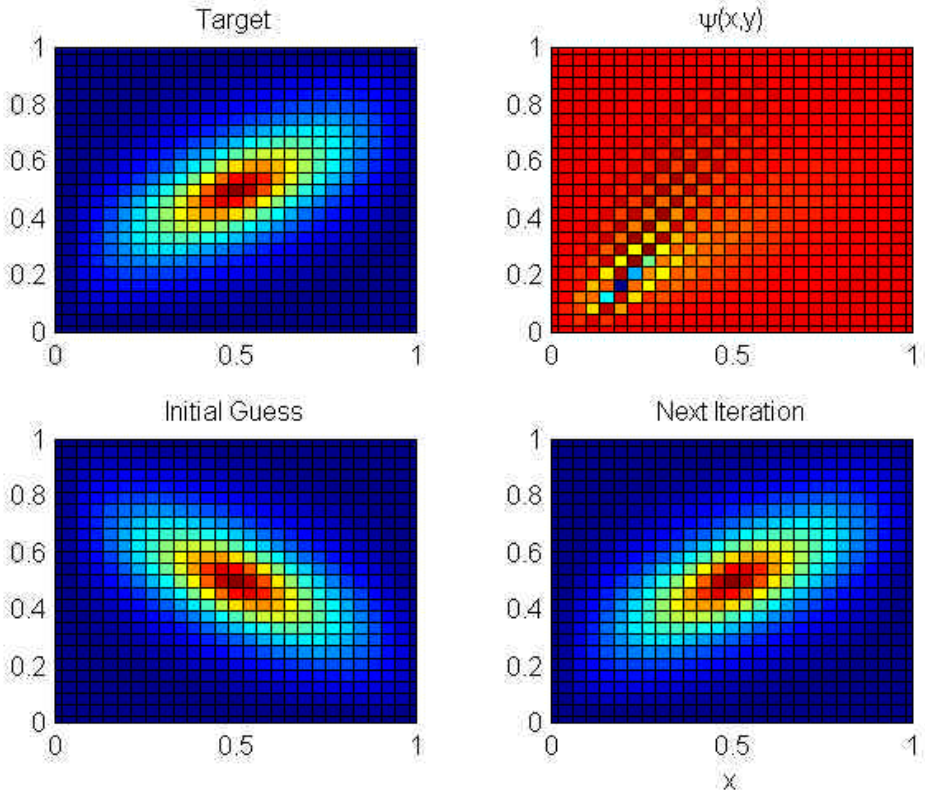

Fig. 8 – The results of permeability tensor computations on a rectangular grid.

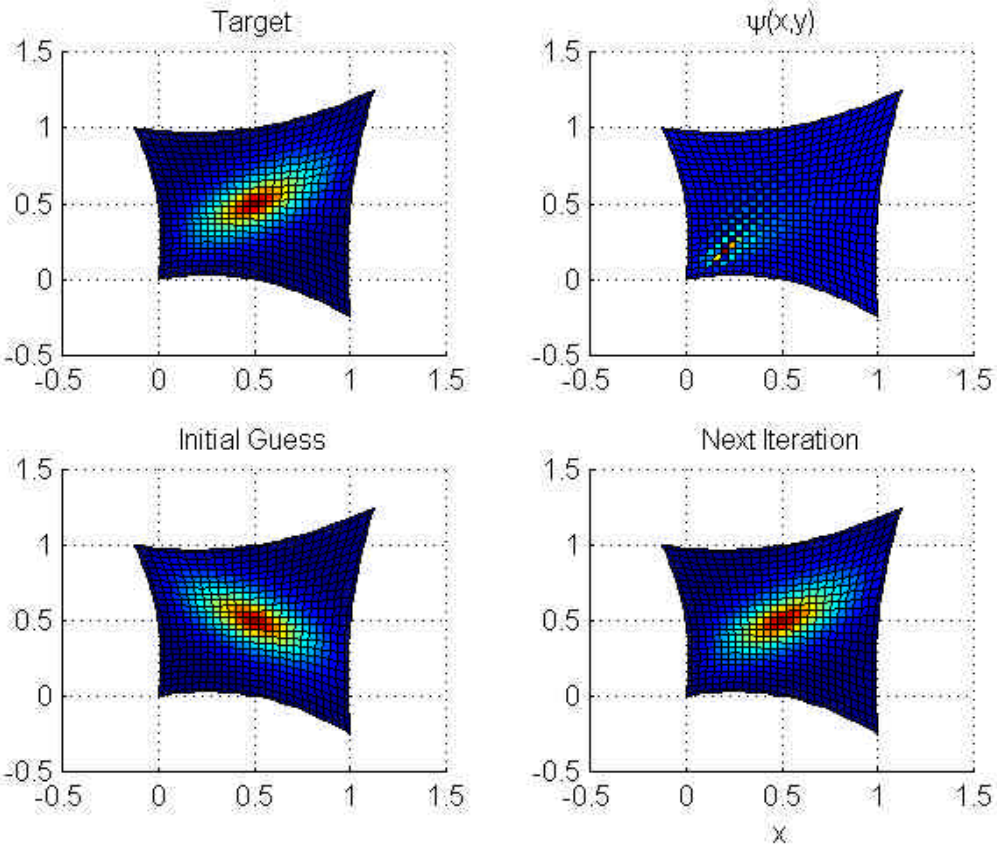

Fig. 9 - The results of computations of permeability tensor on a curvilinear grid 1.

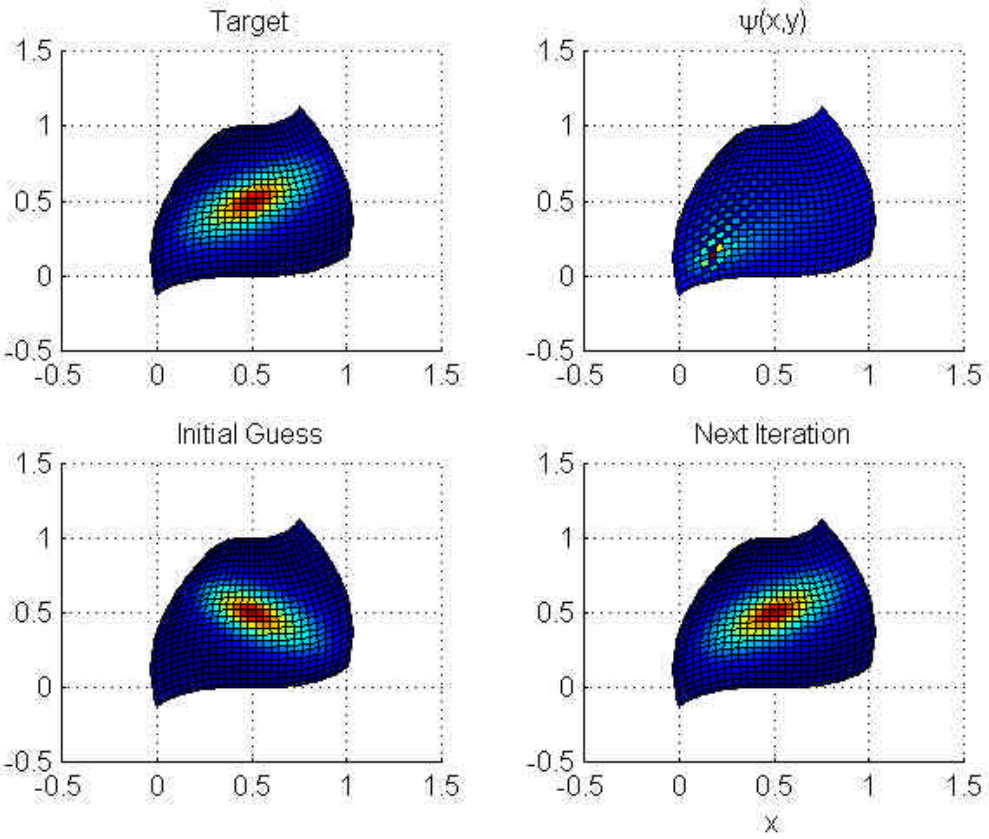

Fig. 10 - Results of computations of permeability tensor on a curvilinear grid 2.